

# RESULTS FROM X-RAY SURVEYS WITH *ASCA*

Yoshihiro Ueda

*Institute of Space and Astronautical Science, Kanagawa 229-8510, Japan*

## ABSTRACT

We present main results from X-ray surveys performed with *ASCA*, focusing on the *ASCA* Large Sky Survey (LSS), the Lockman Hole deep survey, and the *ASCA* Medium Sensitivity Survey (AMSS or the GIS catalog project). The Log  $N$  - Log  $S$  relations, spectral properties of sources, and results of optical identification are summarized. We discuss implications of these results for the origin of the CXB.

KEYWORDS: diffuse radiation — surveys — galaxies: active — X-rays: galaxies

## 1. INTRODUCTION

Understanding the origin of the Cosmic X-ray Background (CXB or XRB) and cosmological evolution of X-ray extragalactic populations is one of the main goals of X-ray astronomy. In the soft X-ray band, the *ROSAT* satellite resolved 80% of the 0.5–2 keV CXB into individual sources (Hasinger *et al.* 1998) and optical identification revealed that the major population is type-I AGNs (Schmidt *et al.* 1998). Because of the technical difficulties, imaging sky surveys in the hard X-ray band (above 2 keV), where the bulk of the CXB energy arises, were not available until the launch of *ASCA*. The sensitivity limits achieved by previous mission such as *HEAO1* (Piccinotti *et al.* 1982) and *Ginga* (Kondo *et al.* 1991) are at most  $\sim 10^{-11}$  erg s $^{-1}$  cm $^{-2}$  (2–10 keV), and the sources observed by them only account for 3% of the CXB intensity in the 2–10 keV band. In particular, there is a big puzzle on the CXB origin, called the “spectral paradox”: bright AGNs observed with *HEAO1*, *EXOSAT* and *Ginga* have spectra with an average photon index of  $\Gamma = 1.7$ –1.9 (e.g., Williams *et al.* 1992), which is significantly softer than that of the CXB itself ( $\Gamma \simeq 1.4$ ; e.g., Gendreau *et al.* 1995). Furthermore, the broad band properties of sources at fluxes from  $\sim 10^{-11}$  to  $\sim 10^{-13}$  erg s $^{-1}$  cm $^{-2}$  (2–10 keV) are somewhat puzzling according to previous studies. The extragalactic source counts in the soft band (0.3–3.5 keV) obtained by *Einstein* Extended Medium Sensitivity Survey (EMSS; Gioia *et al.* 1990) is about 2–3 times smaller than that in the hard band (2–10 keV) obtained by the *Ginga* fluctuation analysis (Butcher *et al.* 1997) when we assume a power-law photon index of 1.7.

The *ASCA* satellite (Tanaka, Inoue, & Holt 1994), launched in 1993 February, was expected to change this situation. It is the first imaging satellite capable of

TABLE 1. Summary of *ASCA* Surveys

Survey Project	Area (deg <sup>2</sup> )	Sensitivity (2–10 keV) (erg s <sup>−1</sup> cm <sup>−2</sup> )
Large Sky Survey (LSS)	7.0	$1.5 \times 10^{-13}$
Deep Sky Survey (DSS)	0.3	$4 \times 10^{-14}$
Lockman Hole Deep Survey	0.2	$4 \times 10^{-14}$
Survey of deep <i>ROSAT</i> fields	1.0	$5 \times 10^{-14}$
<i>ASCA</i> Medium-Sensitivity Survey (AMSS)	110	$7 \times 10^{-14}$

study of the X-ray band above 2 keV with a sensitivity up to several  $10^{-14}$  erg s<sup>−1</sup> cm<sup>−2</sup> (2–10 keV) and covers the wide energy band from 0.5 to 10 keV, which allows us to directly compare results of the energy bands below and above 2 keV with single detectors, hence accompanied with much less uncertainties than previous studies. By taking these advantages, several X-ray surveys have been performed with *ASCA* to reveal the nature of hard X-ray populations: the *ASCA* Large Sky Survey (LSS; Ueda *et al.* 1998), the *ASCA* Deep Sky Survey (DSS; Ogasaka *et al.* 1998; Ishisaki *et al.* 1999 for the Lockman Hole), the *ASCA* Medium-Sensitivity Survey (AMSS or the GIS catalog project: Ueda *et al.* 1997, Takahashi *et al.* 1998, Ueda *et al.* 1999b; see also Cagnoni, Della Ceca, & Maccacaro 1998 and Della Ceca *et al.* 1999), a survey of *ROSAT* deep fields (Georgantopoulos *et al.* 1997; Boyle *et al.* 1998), and so on. The sensitivity limits and survey area are summarized in Table 1. In this paper, we present main results of the *ASCA* surveys, focusing on the LSS (§ 2), the Lockman Hole deep survey (§ 3), and the AMSS (§ 4). In § 5, we summarize these results and discuss their implications for the origin of the CXB.

## 2. THE LARGE SKY SURVEY

### 2.1. X-ray Data

The survey field of the *ASCA* Large Sky Survey (LSS; Ueda *et al.*, 1998) is a continuous region near the north Galactic pole, centered at  $RA(2000) = 13^{\text{h}}14^{\text{m}}$ ,  $DEC(2000) = 31^{\circ}30'$ . Seventy-six pointings have been made over several periods from Dec. 1993 to Jul. 1995. The total sky area observed with the GIS and SIS amounts to  $7.0 \text{ deg}^2$  and  $5.4 \text{ deg}^2$  with the mean exposure time of 56 ksec (sum of GIS2 and GIS3) and 23 ksec (sum of SIS0 and SIS1), respectively. From independent surveys in the total (0.7–7 keV), hard (2–10 keV), and soft (0.7–2 keV) bands, 107 sources are detected with sensitivity limits of  $6 \times 10^{-14}$ ,  $1 \times 10^{-13}$ , and  $2 \times 10^{-14}$  erg s<sup>−1</sup> cm<sup>−2</sup>, respectively. The Log  $N$  - Log  $S$  relations derived from the LSS are summarized in Ueda *et al.* (1999a) together with a complete X-ray source list. At these flux limits,  $30(\pm 3)\%$  of the CXB in the 0.7–7 keV band and  $23(\pm 3)\%$  in the 2–10 keV band have been resolved into discrete sources. The 2–10 keV Log  $N$  - Log  $S$  relation combined with the AMSS result (§4) is plotted in Figure 3.

The spectral properties of the LSS sources suggest that contribution of sources with hard energy spectra become significant at a flux of  $\sim 10^{-13}$  erg s $^{-1}$  cm $^{-2}$  (2–10 keV), which are different from the major population in the soft band. The average 2–10 keV photon index is  $1.49 \pm 0.10$  ( $1\sigma$  statistical error in the mean value) for 36 sources detected in the 2–10 keV band with fluxes below  $4 \times 10^{-13}$  erg s $^{-1}$  cm $^{-2}$ , whereas it is  $1.85 \pm 0.22$  for 64 sources detected in the 0.7–2 keV band with fluxes below  $3 \times 10^{-13}$  erg s $^{-1}$  cm $^{-2}$ . The average spectrum of 74 sources detected in the 0.7–7 keV band with fluxes below  $2 \times 10^{-13}$  shows a photon index of  $1.63 \pm 0.07$  in the 0.7–10 keV range: this index is consistent with the comparison of source counts between the hard and the soft band.

To investigate the X-ray spectra of these hard sources, we made deep follow-up observations with *ASCA* for the five hardest sources in the LSS, selected by the apparent 0.7–10 keV photon index from the source list excluding very faint sources. The results are summarized in Ueda *et al.* (1999c); see also Sakano *et al.* (1998) and Akiyama *et al.* (1998) for AX J131501+3141, the hardest source in the LSS. Three sources in this sample are optically identified as narrow-line AGNs and one is a weak broad-line AGN by Akiyama *et al.* (2000); one is not identified yet. We found that spectra of these sources are most likely subject to intrinsic absorption at the source redshift with column densities of  $N_{\text{H}} = 10^{22} \sim 10^{23}$  cm $^{-2}$ .

## 2.2. Optical Identification

Akiyama *et al.* (2000) summarize the results of optical identification for a sub-sample of the LSS sources, consisting of 34 sources detected in the 2–7 keV band with the SIS. The major advantage of this sample compared with other *ASCA* surveys is good position accuracy; it is 0.6 arcmin in 90% radius from the *ASCA* data alone, thanks to superior positional resolution of the SIS. To improve the position accuracy further, we made follow-up observations with *ROSAT* HRI over a part of the LSS field in Dec. 1997. Optical spectroscopic observations were made using the University of Hawaii 88" telescope, the Calar Alto 3.5m telescope, and the Kitt Peak National Observatories Mayall 4m and 2.1m telescopes.

Out of the 34 sources, 30 are identified as AGNs, 2 are clusters of galaxies, 1 is a Galactic star, and only 1 object remains unidentified. The identification as AGNs is based on existence of a broad emission line or the line ratios of narrow emission lines ([NII]6583Å/H $\alpha$  and/or [OIII]5007Å/H $\beta$ ); see Akiyama *et al.* 2000 and references therein. Figure 1(a) shows the correlation between the redshift and the apparent photon index in the 0.7–10 keV range, which is obtained from a spectral fit assuming no intrinsic absorption, for the identified objects. The 5 sources that have an apparent photon index smaller than 1.0 are identified as 4 narrow-line AGNs and 1 weak broad-line AGN, all are located at redshift smaller than 0.5. On the other hand, X-ray spectra of the other AGNs are consistent with those of nearby type 1 Seyfert galaxies. Four high redshift broad-line AGNs show somewhat apparently hard spectra with an apparent photon index of  $1.3 \pm 0.3$ , although it may be still marginal due to the limited statistics.

To avoid complexity in classifying the AGNs by the optical spectra, we divide the identified AGNs into two using the X-ray data: the “absorbed” AGNs which show intrinsic absorption with a column density of  $N_{\text{H}} > 10^{22} \text{ cm}^{-2}$  and the “less-absorbed” AGNs with  $N_{\text{H}} < 10^{22}$ . Correcting the *flux* sensitivity for different X-ray spectra, we found the contribution of the absorbed AGNs is almost comparable to that of less-absorbed AGNs in the 2–10 keV source counts at a flux limit of  $2 \times 10^{-13} \text{ erg s}^{-1} \text{ cm}^{-2}$ . Figure 1(b) shows the correlation between the redshift and the 2–10 keV luminosity of the identified AGNs. The redshift distribution of the 5 absorbed AGNs is concentrated at  $z < 0.5$ , which contrasts to the presence of 15 less-absorbed AGNs at  $z > 0.5$ . This suggests a deficiency of AGNs with column densities of  $N_{\text{H}} = 10^{22-23}$  at  $z = 0.5-2$ , or in the X-ray luminosity range larger than  $10^{44} \text{ erg s}^{-1}$ , or both. Note that if the 4 broad-line AGNs with hard spectra have intrinsic absorption instead of other hardening mechanism such as Compton reflection, it could complement this deficiency.

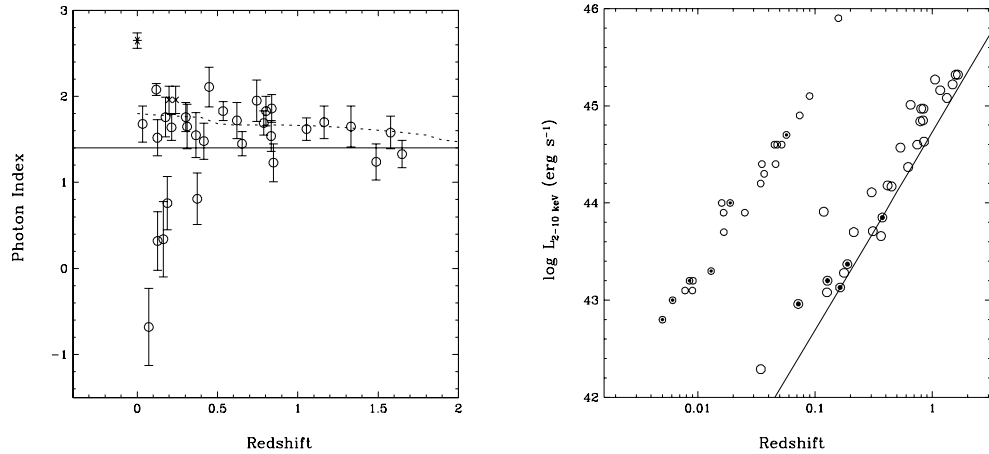


FIGURE 1. (a) left: the correlation between the redshift and the apparent 0.7–10 keV photon index for the identified objects in the LSS (Akiyama *et al.* 2000). The open circles, crosses, and asterisk represent AGNs, clusters of galaxies, and a Galactic star, respectively. The dotted curve shows the expected apparent photon index in the observed 0.7–10 keV band as a function of redshift, for a typical spectrum of type-1 Seyfert galaxies with a Compton reflection component. (b) right: The 2–10 keV luminosity versus redshift diagram for the LSS AGNs (with large open circles, Akiyama *et al.* 2000), and for the *HEAO1A2* AGNs (with small marks, Piccinotti *et al.* 1982). The “absorbed” AGNs are plotted with dots. Lines indicate detection limits of the LSS for a source with an photon index of 1.7 with no intrinsic absorption.

### 3. THE LOCKMAN HOLE DEEP SURVEY

Deep surveys were performed with *ASCA* over several fields (Ogasaka *et al.* 1998), although optical identification is more difficult than the LSS because of faint flux levels and source confusion problem. To overcome this difficulty, we have been conducting a deep survey of the Lockman Hole, where the *ROSAT* deep survey was performed (Hasinger *et al.* 1998). The advantage of selecting this field is that we already have a complete soft X-ray source catalog down to a flux limit of  $5.5 \times 10^{-15}$  erg s $^{-1}$  cm $^{-2}$  (0.5–2 keV), most of which have been optically identified (Schmidt *et al.* 1998). In addition, we utilized an X-ray source list at even fainter flux limits (G. Hasinger, private communication). Since the flux limits of the *ROSAT* surveys are extremely low, we can expect most of *ASCA* sources could have *ROSAT* counterparts within reasonable range of spectral hardness. Utilizing positions of the *ROSAT* sources, we can determine the hard-band flux for individual sources, which would otherwise have been difficult to separate, to a flux limit of  $3 \times 10^{-14}$  erg s $^{-1}$  cm $^{-2}$  (2–10 keV). Preliminary results are reported in Ishisaki *et al.* (1999).

Up to present, we have made 3 pointings in the direction of the Lockman Hole with *ASCA* on 1993 May 22–23, 1997 April 29–30, and 1998 November 27 for a net exposure of 63 ksec (average of the 8 SIS chips), 64 ksec, and 62 ksec, respectively. The pointing positions were arranged so that the superposed image of the SIS field of views (FOVs) covers the PSPC and HRI FOVs as much as possible. We here used only the SIS data considering its superior positional resolution. Analysis was made through the 2-dimensional maximum-likelihood fitting to a raw, superposed image in photon counts space in the sky coordinates, with a model consisting of source peaks (point spread functions) and the background. As a first step, we put sources into the model at the positions of the *ROSAT* catalogs. Then, after checking the residual image of the fit, we added remaining peaks that were missing in the *ROSAT* catalogs. Thus, we determined the significance and flux of each source in three energy bands, 0.7–7 keV, 2–7 keV, and 0.7–2 keV, including new sources detected with *ASCA*. We corrected for the degradation of detection efficiency caused by the radiation damage using the CXB intensity. Note that the *ASCA* sensitivity limits strongly depends on position due to the multiple pointings and the vignetting of the XRT.

We detected 27 sources altogether with significances higher than  $3.5\sigma$  in either of the three survey bands. Two sources were newly detected with *ASCA*. One object is a variable source having a 0.7–7 keV photon index of about 1.7, which was very faint during the *ROSAT* observations. The other shows a very hard spectrum and is detected only in the 2–7 keV band. In the combined SIS FOVs, 43 sources out of 50 sources in the Schmidt *et al.* (1998) catalog are located. Identification of *ASCA* sources using the *ROSAT* catalog is summarized in Table 2. Since the number of sources detected in the 2–7 keV band is limited due to poor photon statistics, we here use the results for 25 sources detected in the 0.7–7 keV band for comparison with the *ROSAT* survey. Four unidentified sources in the *ASCA* survey have *ROSAT* counterparts in the deeper X-ray source catalog (G. Hasinger, private

TABLE 2. Summary of optical identification of the *ASCA* Lockman Hole deep survey by the *ROSAT* catalog (Schmidt *et al.* 1998)

Population	<i>ROSAT</i>	<i>ASCA</i> (0.7–7 keV)
Total	43	25
Type-1 AGN (a-c)	26	13
Type-2 AGN (d-e)	7	6
Group/Galaxies	3	0
Star	3	1
Unidentified	4	4+1

communication) and remaining one is the variable source detected only with *ASCA*. For AGNs identified by Schmidt *et al.* (1998), we divided them into two according to their optical spectra: (1) type-1 AGNs, corresponding to either of class a, b, or c, showing broad emission lines, and (2) type-2 AGN, class d or e, showing only narrow emission lines. As noticed from the table, 6 out of 7 type-2 AGNs were detected, whereas only half of the 26 type-1 AGNs were detected with *ASCA*, which covers much harder band than the *ROSAT*. This suggests that contribution of type-2 AGNs are more dominant in higher energy bands than in the soft band at similar flux levels.

#### 4. THE *ASCA* MEDIUM-SENSITIVITY SURVEY

Because these surveys are limited in sky coverage, the sample size is not sufficient to obtain a self-consistent picture about the evolution of the sources over the wide fluxes, from  $\sim 10^{-11}$  erg s $^{-1}$  cm $^{-2}$  (2–10 keV) which is the sensitivity limit of *HEAO1* A2 (Piccinotti *et al.* 1982), down to  $\sim 10^{-13}$  erg s $^{-1}$  cm $^{-2}$  (2–10 keV), that of *ASCA*. To complement these shortcomings, we have been working on the project called the “*ASCA* Medium Sensitivity Survey (AMSS)”, or the GIS catalog project. In the project, we utilize the GIS data from the fields that have become publicly available to search for serendipitous sources. The large field of view and the low-background characteristics make the GIS instrument ideal for this purpose.

Main results from the AMSS are reported in Ueda *et al.* (1999b), which were obtained from selected GIS fields of  $|b| > 20^\circ$  observed from 1993 to 1996, covering the total sky area of 106 deg $^{-2}$ . The sample contains 714 serendipitous sources, of which 696, 323, and 438 sources are detected in the 0.7–7 keV (total), 2–10 keV (hard), and 0.7–2 keV (soft) band, respectively. This is currently the largest X-ray sample covering the 0.7–10 keV band. Figure 2(a) shows the correlation between the 0.7–7 keV flux and the hardness ratio between the 2–10 keV and 0.7–2 keV count rates. We also plot the average hardness ratio in several flux ranges, separated by the dashed curves, with crosses. It is clearly seen that the average spectrum becomes harder with a decreasing flux: the corresponding photon index (assuming

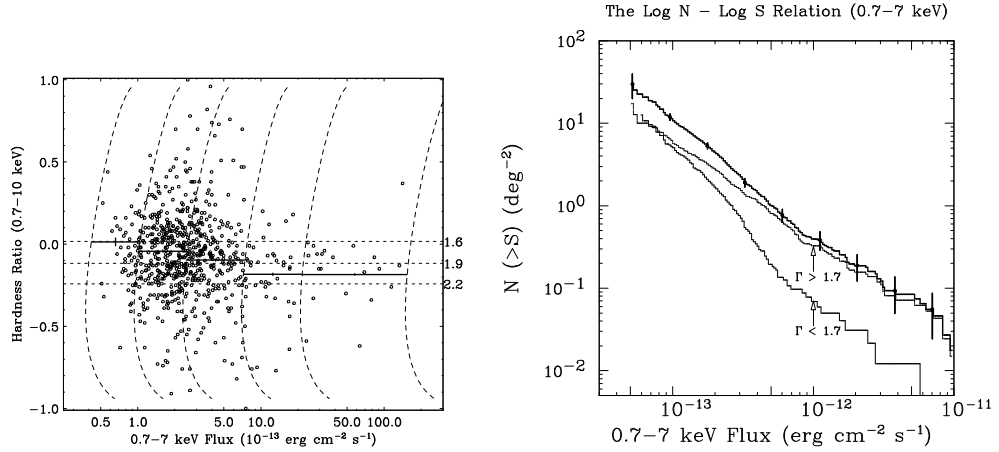


FIGURE 2. (a) left: The correlation between the 0.7–7 keV flux and the hardness ratio between the 0.7–2 keV and 2–10 keV count rates for sources detected in the 0.7–7 keV survey in the AMSS sample (Ueda *et al.* 1999b). The crosses show the average hardness ratios (with  $1\sigma$  errors in the mean value) in the flux bin separated by the dashed curves, at which the count rate hence the sensitivity limit is constant. The dotted lines represent the hardness ratios corresponding to a photon index of 1.6, 1.9, and 2.2 assuming a power law spectrum. (b) right: The integral  $\log N$  -  $\log S$  relations in the 0.7–7 keV survey band, derived from the AMSS sample. The medium-thickness curve represents the result for the hard source sample, consisting of sources with an apparent 0.7–10 keV photon index  $\Gamma$  smaller than 1.7, the thin curve represents that for the soft source sample (with  $\Gamma$  larger than 1.7), and the thick curve represents the sum. The 90% statistical errors in source counts are indicated by horizontal bars at several data points.

a power law over the 0.7–10 keV band with no absorption) changes from 2.1 at the flux of  $\sim 10^{-11}$   $\text{erg s}^{-1} \text{cm}^{-2}$  to 1.6 at  $\sim 10^{-13}$   $\text{erg s}^{-1} \text{cm}^{-2}$  (0.7–7 keV). Similar hardening are also reported in the 2–10 keV range by Della Ceca *et al.* (1999) using 60 serendipitous sources. Figure 2(b) shows the integral  $\log N$  -  $\log S$  relations in the 0.7–7 keV survey band for the soft source sample, consisting of sources with an apparent 0.7–10 keV photon index larger than 1.7, and for the hard source sample, with an index smaller than 1.7. This demonstrates that sources with hard energy spectra in the 0.7–10 keV range are rapidly increasing with decreasing fluxes, compared with softer sources.

## 5. SUMMARY

The *ASCA* surveys have brought a clear, self-consistent picture about statistical properties of sources that constitute about 30% of the CXB in the broad energy

band of 0.7–10 keV. Figure 3 summarizes the 2–10 keV Log  $N$  - Log  $S$  relation obtained from the *ASCA* surveys together with the results from previous missions. The direct source counts from combined results of the LSS (Ueda *et al.* 1999b) and the AMSS (Ueda *et al.* 1999c; these contain the data used by Cagnoni, Della Ceca, & Maccacaro 1998) give the tightest constraints so far over a wide flux range from  $\sim 10^{-11}$  to  $\sim 7 \times 10^{-14}$  erg s $^{-1}$  cm $^{-2}$ :  $N(> S) = 16.8 \pm 7.2$  (90% statistical error),  $11.43 \pm 2.4$ ,  $3.76 \pm 0.42$ ,  $1.08 \pm 0.17$ , and  $0.33 \pm 0.09$  deg $^{-2}$ , at  $S = 7.4 \times 10^{-14}$ ,  $1.0 \times 10^{-13}$ ,  $2.0 \times 10^{-13}$ ,  $4.0 \times 10^{-13}$ , and  $1.0 \times 10^{-12}$  erg s $^{-1}$  cm $^{-2}$ , respectively. The DSS gives a direct source counts at the faintest flux,  $3.8 \times 10^{-14}$  erg s $^{-1}$  cm $^{-2}$  (Ogasaka *et al.* 1998), whereas the fluctuation analysis of deep SIS fields constrains the Log  $N$  - Log  $S$  relation at fluxes down to  $1.5 \times 10^{-14}$  (Gendreau, Barcons, & Fabian 1998). As seen from the figure, the *ASCA* direct source counts smoothly connect the two regions constrained by the *Ginga* and *ASCA* fluctuation analysis.

The AMSS/LSS results demonstrate that the average spectrum of X-ray sources becomes harder toward fainter fluxes: the apparent photon index in the 0.7–10 keV range changes from 2.1 at the flux of  $\sim 10^{-11}$  to 1.6 at  $\sim 10^{-13}$  erg s $^{-1}$  cm $^{-2}$  (2–10 keV). This fact can be explained by the rapid emergence of population with hard energy spectra, as is clearly indicated in Figure 2(b). The evolution of broad-band properties of sources solves the puzzle of discrepancy discrepancy of the source counts between the soft (EMSS) and the hard band (*Ginga* and *HEAO1*). If we compare the *ASCA* Log  $N$  - Log  $S$  relations (including Galactic objects) between above and below 2 keV, the hard band source counts at  $S \sim 10^{-13}$  erg s $^{-1}$  cm $^{-2}$  (2–10 keV) matches the soft band one when we assume a photon index of 1.6 for flux conversion, whereas at brighter level of  $S = 4 \times 10^{-13} \sim 10^{-12}$  erg s $^{-1}$  cm $^{-2}$  (2–10 keV), we have to use a photon index of about 1.9 to make them match. The latter fact is consistent with the average 0.7–10 keV spectrum at the same flux levels, and can be connected the the “soft” spectrum of the fluctuation observed with *Ginga*, which shows a photon index of  $1.8 \pm 0.1$  in the 2–10 keV range (Butcher *et al.* 1997).

The optical identification revealed that the major population at fluxes of  $10^{-13}$  erg s $^{-1}$  cm $^{-2}$  are AGNs. The population of hard sources, which are most responsible for making the average spectrum hard, are X-ray absorbed sources. They are mostly identified as narrow line (type-2) AGNs. The contribution of these type-2 AGNs is larger in the hard band than in the soft band at the same flux limit. Recent results of the 5–10 keV band survey by *BeppoSAX* confirms this tendency (Fiore *et al.* 1999). These results support the scenario that the CXB consists of unabsorbed AGNs and absorbed AGNs, whose contribution becomes more significant with decreasing fluxes and in harder energy band.

We found, however, possible evidence that is not consistent with the “unified scheme” of AGNs (e.g., Awaki *et al.* 1991), on which many AGN synthesis models are based. The LSS results may imply deficiency of X-ray luminous, absorbed AGNs, with  $N_{\text{H}} = 10^{22-23}$  at  $z = 0.5-2$ , or in the X-ray luminosity range larger than  $10^{44}$  erg s $^{-1}$ , although we cannot rule out possibility, for example, that there are many luminous AGNs at  $z > 2$  with extreme heavy absorption of  $N_{\text{H}} > 10^{24}$ . On the other hand, there is another implication that there could be a population of AGNs

at high redshifts ( $z > 1$ ) that are optically identified as type-1 AGNs but have apparently hard X-ray spectra, although the origin of the hardness is not clear yet. Future surveys by *Chandra* and *XMM* together with optical identification of the AMSS sources will reveal the luminosity, number, and spectral evolutions of extragalactic populations including absorbed AGNs, which will eventually lead us to full understanding of the origin of the CXB.

#### ACKNOWLEDGEMENTS

I thank all the collaborators of our *ASCA* survey projects, especially, M. Akiyama, G. Hasinger, H. Inoue, Y. Ishisaki, I. Lehmann, K. Makishima, Y. Ogasaka, T. Ohashi, K. Ohta, M. Sakano, T. Takahashi, T. Tsuru, W. Voges, T. Yamada, and A. Yamashita.

#### REFERENCES

Akiyama, M., *et al.* 1998, ApJ, 500, 173  
 Akiyama, M., *et al.* 2000, ApJ, in press  
 Awaki, H., Koyama, K., Inoue, H., & Halpern, J.P. 1991, PASJ, 43, 195  
 Boyle, B.J., *et al.* 1998, MNRAS, 296, 1  
 Butcher, J.A., *et al.* 1997, MNRAS, 291, 437  
 Cagnoni, I., Della Ceca, R., & Maccacaro, T. 1998, ApJ, 493, 54  
 Della Ceca, R., *et al.* 1999, ApJ, 524, 674  
 Fiore, F., *et al.* 1999, MNRAS, 306, L55  
 Gendreau, K.C., *et al.* 1995, PASJ, 47, L5  
 Gendreau, K.C., Barcons, X., & Fabian, A.C. 1998, MNRAS, 297, 41  
 Georgantopoulos, I., *et al.* 1997, MNRAS, 291, 203  
 Gioia, I.M. *et al.* 1990, ApJS, 72, 567  
 Hasinger, G. 1998, AN, 319, 37  
 Hasinger, G., *et al.* 1998, A&A, 329, 482  
 Ishisaki, Y., *et al.* 1999, Advanced in Space Research, in press  
 Kondo, H. *et al.* 1982, in “Frontiers of X-ray Astronomy”, Universal Academy Press, Tokyo, p.655  
 Ogasaka, Y., *et al.* 1998, Astro. Nachr., 319, 43  
 Piccinotti, G., *et al.* 1982, ApJ, 253, 485  
 Sakano, M. *et al.* 1998, ApJ, 505, 129  
 Schmidt, M., *et al.* 1998, A&A, 329, 495  
 Takahashi, T., Ueda, Y., Ishisaki, Y., Ohashi, T., & Makishima, K. 1998, AN, 319, 91  
 Tanaka, Y., Inoue, H., & Holt, S.S. 1994, PASJ, 46, L37  
 Ueda, Y., Takahashi, T., Ishisaki, Y., Makishima, K. & 1997, in “All-Sky X-Ray Observations in the Next Decade”, RIKEN, Saitama, p55  
 Ueda, Y., *et al.* 1998, Nature, 391, 866  
 Ueda, Y., *et al.* 1999a, ApJ, 518, 656  
 Ueda, Y., Takahashi, T., Ishisaki, Y., Ohashi, T., & Makishima, K. 1999b, ApJ, 524, L11  
 Ueda, Y., *et al.* 1999c, Advanced in Space Research, in press  
 Williams, O.R. *et al.* 1992, ApJ, 389, 157

### The Log N – Log S Relation (2–10 keV)

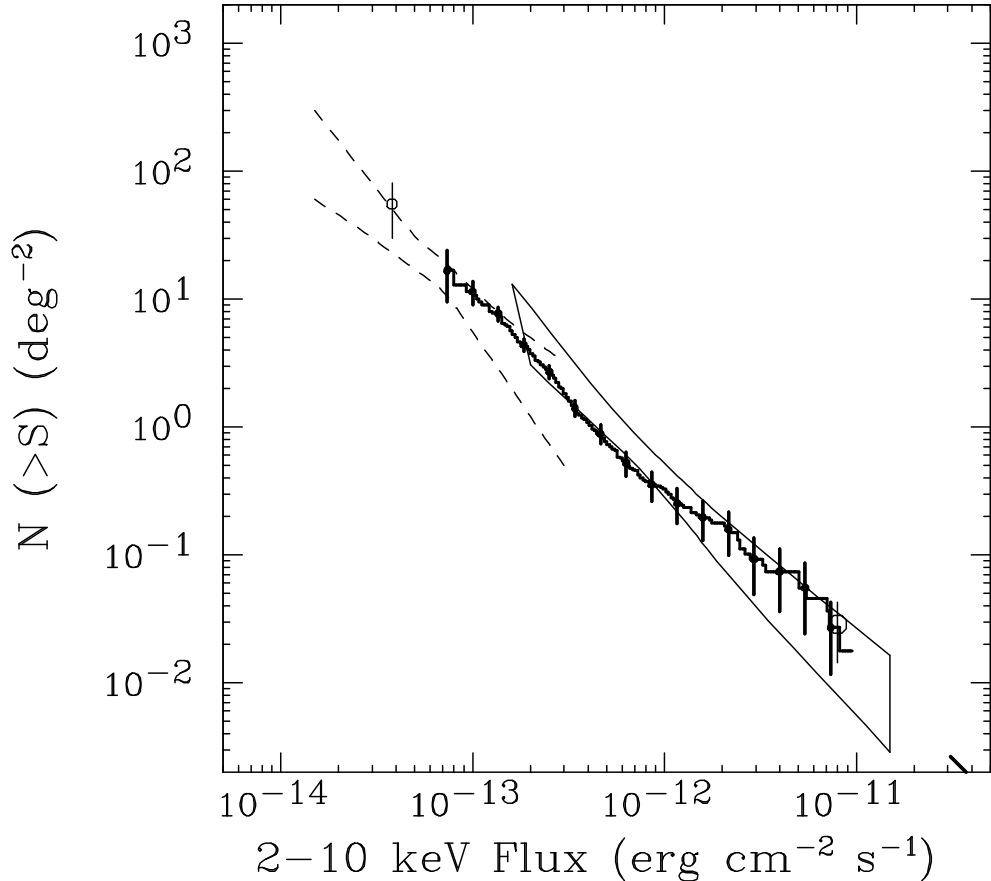


FIGURE 3. Summary of the 2–10 keV Log  $N$  - Log  $S$  relation obtained by the *ASCA* surveys, compared with previous results. The steps are the combined results from the LSS (Ueda *et al.* 1998) and the AMSS (Ueda *et al.* 1999b). The faintest point at  $4 \times 10^{-14} \text{ erg s}^{-1} \text{ cm}^{-2}$  is derived from the DSS utilizing the SIS data (Ogasaka *et al.* 1998). The trumpet shape between two dashed lines indicates  $1\sigma$  error region from the fluctuation analysis of *ASCA* SIS deep fields (Gendreau, Barcons & Fabian 1998). The contour at  $10^{-13} \sim 10^{-11} \text{ erg s}^{-1} \text{ cm}^{-2}$  represents the constraints by the *Ginga* fluctuation analysis at 90% confidence level (Butcher *et al.* 1997). The open circle at  $8 \times 10^{-12} \text{ erg s}^{-1} \text{ cm}^{-2}$  corresponds to the source count by *Ginga* survey (Kondo *et al.* 1991), and the thick-line above  $3 \times 10^{-11} \text{ erg s}^{-1} \text{ cm}^{-2}$  is the extragalactic Log  $N$  - Log  $S$  relation determined by *HEAO1 A2* (Piccinotti *et al.* 1982). All the horizontal bars represent 90% statistical errors in source counts.